Journal Name

ARTICLE

Americium incorporation into studtite

Saptarshi Biswas,[a] Samuel Edwards,[a] Zheming Wang,[b] Hang Si,[c] Luis León Vintró,[d] Brendan Twamley,[a] Piotr M. Kowalski[c] and Robert J. Baker[a]

Received 00th January 20xx,
Accepted 00th January 20xx

DOI: 10.1039/x0xx00000x

www.rsc.org/

Abstract text goes here. The abstract should be a single paragraph that summarises the content of the article

Introduction

The safe storage of highly radioactive spent nuclear fuels is a complex challenge that requires the underpinning chemistry to be well understood. The current policy in the EU is to store this waste in a suitably engineered underground repository for 10^6 years.[1] Under reducing conditions uraninite (UO_{2+x}) or coffinite ($USiO_4$) are the dominant minerals that would be formed, but a study of the chemistry of coffinite has been hampered by the difficulty in synthesising pure material.[2] Under oxidizing conditions, that could be localised, UO_2, the major component of spent nuclear fuels (SNF), is thermodynamically unstable and will oxidise to UO_3 via a number of phase transitions containing the uranyl ion, some of which have been experimentally characterised.[3] This controls the solubility, and thus mobility, of uranium in the environment. Interestingly, these phases interact with other radionuclides via a number of mechanisms and can inhibit or accelerate their mobility. The most studied radioisotope is neptunium, as Np(V) is very soluble in groundwater with low adsorption onto the geomatrix[4] which, combined with a high radiotoxicity, makes it especially important to understand the underlying chemistry. The mechanism(s) of incorporation are still uncertain, but a charge balancing substitution of $[NpO_2]^+$ and M^+ for $[UO_2]^{2+}$ has been postulated for a number of minerals[5] whilst co-precipitation of a distinct Np_2O_5 phase[6] or direct substitution[7] of $[UO_2]^{2+}$ for $[NpO_2]^{2+}$ has also been observed.

Based on an analysis of the crystal chemistry of uranyl minerals, it was predicted that the substitution of An(III) (An = Pu, Am, Cm) may occur either at the interlayer sites or in the sheets of minerals,[8] as has been observed with Np(V). Whilst americium is not a major principle component of SNF (ca. 0.06 wt. %), decay of ^{241}Pu, which is a significant fraction of irradiated fuel, means that ^{241}Am is a grow-in product. Current calculations suggest 594g Am (as 503g ^{241}Am, 0.66g ^{242m}Am and 90.6g ^{243}Am, or 64.5 TBq of radiation) per metric ton of uranium will be present after 10 year decay.[9] Therefore, the build-up of Am becomes extremely significant for the later timeframe. Due to the high specific activity of this isotope, and the fact that the +3 oxidation state dominates for Am under environmental conditions,[10] little has been reported on this topic. Am(III) sorption and incorporation studies have been reported on minerals such as calcite ($CaCO_3$), aluminium or iron oxides and hydroxides or clay materials.[11] We recently described a series of uranyl minerals that uptake that Am(III) from solution and characterised them by vibrational and photoluminescence spectroscopy.[12] The nature of the uranyl phase determines the amount of Am(III) uptake into the solid and uranyl carbonates are favoured over oxyhydroxides. In contrast studtite, $[UO_2(\eta^2\text{-}O_2)(H_2O)_2]\cdot 2H_2O$, does not incorporate ^{241}Am(III) on tracer scales,[13] in keeping with earlier investigations of meta-studtite, $[UO_2(\eta^2\text{-}O_2)(H_2O)_2]$, on the surface of SNF.[14] Metastudtite is the thermodynamically stable mineral as dehydration is irreversible.[15] Both these phases have been found in UO_2[16] or SNF[14] exposed to water or even in the oxidative corrosion of

[a] School of Chemistry, University of Dublin Trinity College, Dublin 2, Ireland. Email: bakerrj@tcd.ie
[b] Pacific Northwest National Laboratory, MSIN K8-96, P.O. Box 999, Richland, WA 99352, United States.
[c] Institute of Energy and Climate Research, IEK-6: Nuclear Waste Management and Reactor Safety, Forschungszentrum Jülich GmbH, Wilhelm-Johnen-Strasse, 52428 Jülich, Germany.
[d] School of Physics, University College Dublin, Belfield, Dublin 4, Ireland
† Footnotes relating to the title and/or authors should appear here.
Electronic Supplementary Information (ESI) available: Further spectroscopic and structural data. See DOI: 10.1039/x0xx00000x

depleted uranium munitions.[17] Moreover a number of other mineral phases, e.g. oxyhydroxides, are converted to studtite in the presence of hydrogen peroxide.[18] Thus, given its ease of formation, studtite has been studied for radionuclide sorbtion. For example, Sr^{2+} and Cs^{+} are formed as surface sorbed species,[19] whilst Np, either as the +5 or +6 oxidation states, is also incorporated into the structure.[20] However, the concentrations of Np in these experiments were very low, so it is difficult to assign oxidation states and where the Np is located is open to debate. Given the interesting chemistry of Np we reasoned that if the radionuclide is incorporated into the structure, specifically a replacement of a uranyl moiety for a $[NpO_2]^{n+}$, and given the instability of the americinyl(V) ion to reduction,[21] if $[AmO_2]^{+}$ were treated with studtite and incorporation occurred, subsequent reduction to Am(III) would trap this in the chains. Herein we report on tracer studies of Am incorporations and spectroscopic assignment of the Am(III) oxidation state. A computational study to explore the energetics of incorporation of selected actinides (An = Np, Am) in different oxidation states (+4 to +6) is also presented.

Results and Discussion

The synthesis of studtite was firstly examined as a function of pH and powder XRD afforded a degree of crystallinity to be calculated. The starting material appears to be important as uranyl acetate consistently gave poorly crystalline material. Uranyl nitrate did give material that was crystalline, and the pH also determines the yield (Table 1), and is in line with solubility studies reported previously.[22] It is noteworthy that in the X-ray beam, studtite was rapidly dehydrated to metastudtite, so our measurements were conducted in sealed capillaries at -40 °C.

Americinyl solutions were prepared via the literature method.[23] We tried two methods for incorporation namely synthesis of studtite in the presence of $[AmO_2]^{+}$ (a co-precipitation method) and a contacting procedure using a solution of 50 Bq Am(V) and studtite at different pH overnight. The resulting yellow precipitate was isolated, washed with water and dried. The amount of Am was quantified by γ-spectrometry (Table 2). Whilst the activity in the sample is low, it is clear that the pH does not significantly affect the amount of Am in the solids. Using a higher concentration of Am for the coprecipitation methodology at pH 5 afforded a low yield (~10%) of a yellow powder that was also quantified by γ-spectrometry (Table 2). Comparison of *D* (the distribution ratio, or the ratio between the americium activity in the solid and solution) shows the uptake to be low but consistent between methodologies.

This method does not give any information on the speciation of the americium, so we have measured the Raman spectra and the solid-state emission spectra to attempt to gain insight into the oxidation state and local environment. The Raman spectra of the contacted and incorporated methodology are similar but compared to pure studtite there are some small shifts in both the uranyl (818 cm^{-1}) and peroxo (864 cm^{-1}) stretches. Notably there is a small ν(U=O) peak at the same frequency of studtite (834 cm^{-1}) in both methods, which is larger for the contacted methodology. Using the

Table 1. Yield and crystallinity of studtite prepared at different pH.

pH	% yield	% crystallinity
1.4	62	79
2.5	90	44
4.7	100	47
5.5	87	64
6.5	80	80

Table 2. Quantification of ^{241}Am in solid and solution samples.

pH	Activity in solid Bq/mg	Activity in liquid Bq/mL	*D* (x 10^{-3})
1.0	0.157	32	4.84
3.0	0.179	43	4.15
5.0	0.104	41	2.25
coprecipitation	1.34	584	1.94

formula developed by Bartlett and Cooney[24] which relates the vibrational frequency to the bond length, the U=O elongates from 1.781 Å in studtite (from the X-ray structure $d_{(U=O)}$ = 1.768(7) Å)[25] to 1.792 Å in Am incorporated studtite. There is no evidence of the Am^{V}=O stretch which appears at approx. 730 cm^{-1}.[21] Vibrational spectroscopy suggests that the Am is in its +3 oxidation state and to validate this, photoluminescence measurements were recorded on a contacted solid at room temperature and the coprecipitation product at room temperature; the emission spectra are shown in Fig 2. There are no reports of the emissive behaviour of any compounds of Am(V) or Am(VI). Those of Am(III) are scarce but two transitions can be generally observed: $^5D_1 \rightarrow {}^7F_J$ (J = 1, 2) at ca. 700 and 840 nm respectively, with the former somewhat diagnostic. For instance, in the aqua complex λ_{em} = 685 nm whilst for the carbonate complex $[Am(CO_3)_3]^{3-}$ this maxima shifts to 693 nm[26] and we have shown that Am(III) in uranyl oxyhdroxides and uranyl carbonates λ_{em} = 687 nm.[12] In the contacted studtite sample, a broad peak centred at λ_{em} = 683 nm suggests that the Am is hydrated but we were unable to measure the lifetimes to confirm the degree of hydration. Furthermore we were able to resolve the weak $^5D_1 \rightarrow {}^7F_2$ transition centred at λ_{em} = 827 nm. Interestingly, a shift is observed to λ_{em} = 686 nm in the coprecipitation methodology and the transition to the $^7F_2$ level was not observed. These spectroscopic results suggest that the Am(V) has been reduced to Am(III) which changes the local coordination environment of the uranyl ion and the peroxo group, but that the emission spectra shows the speciation is different from the two methodologies. Finally, it is worth noting that the emission

Charge compensation mechanism	Actinide	Studtite incorporation energy (eV)	metastudtite incorporation energy (eV)
M1	Np	1.42	1.35
	Am	2.50	2.51
M2	Np	2.49	2.16
	Am	3.19	3.98
M3	Np	3.01	3.18
	Am	4.34	3.95

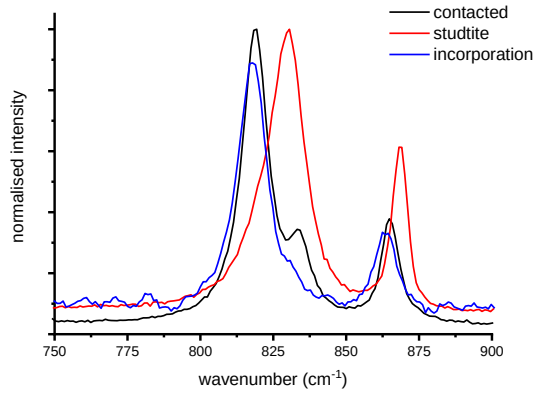

Figure 1. Raman spectra for studtite and the precipitates from Am co-precipitation and contacting.

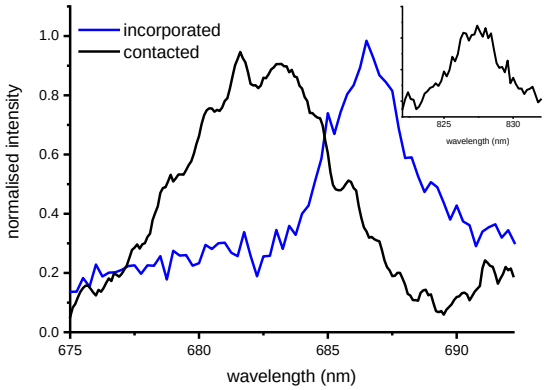

Figure 2. Raman spectra for studtite and the precipitates from Am co-precipitation and contacting.

spectra were measured at λ_{ex} = 380 nm and we see no bands due to the uranyl emission; sensitised emission of the Am(III) was observed in our uranyl oxyhydroxide and carbonate examples.

Spectroscopic evidence clearly showed the presence of Am(III) but to investigate the stabilities further we have turned to computational chemistry as it has been shown that this can be useful guide to the An incorporation chemistry of studtite[27] and other mineral phases.[28] The calculations were performed with DFT+*U* method to account for the *5f* electrons correlation effects. The Hubbard *U* parameters were 2.5 eV and 3.1 eV for Am and Np atoms, respectively, taken from our previous work.[29] We firstly computed the incorporation energies of both Np and Am into studtite and metastudtite phases with a composition of $U_{0.75}An_{0.25}$, taking the respective AnO_2 as reference phases. To find the most preferable charge compensation mechanism we followed earlier work on Np incorporation, [30] and computed the incorporation of Np(V) and Am(V) assuming charge compensation by: (M1) hydrogen attached to the *An*-yl oxygen, (M2) the formation of OH_3^- anion through adding hydrogen to a water molecule and (M3) the formation of an oxygen vacancy. The resultant incorporation

Table 3. The energy (in eV) of An(V) incorporation into studtite (ST) and metastudtite (MST) through three charge compensation mechanisms, as discussed in the text.

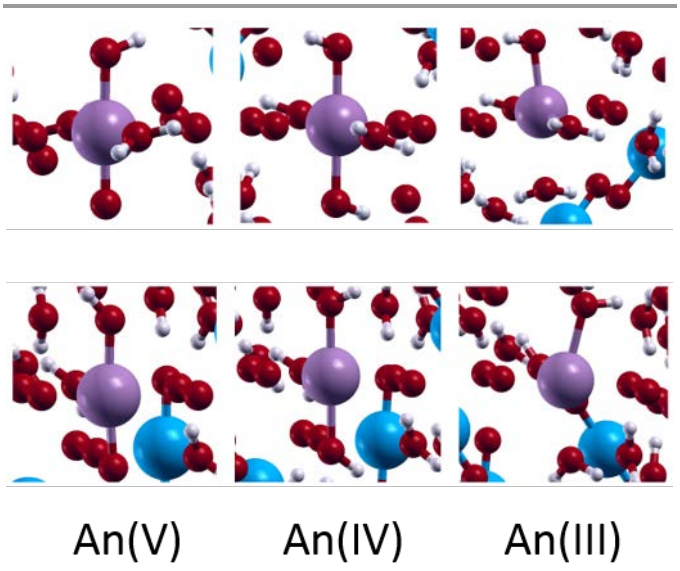

Fig. 3. Incorporation configurations of An(V), An(IV) and An(III) into studtite (top) and metastudtite (bottom), explicitly showing the charge balancing hydrogen atom.

energies are given in Table 3. In both cation cases the preferred charge compensation mechanism is by attachment of H atom to the -yl oxygen, as shown in Reaction 1 where *S* indicates the studtite or metastudtite solid phase and *An* = Np, Am.

$$S + AnO_2 + 1/2n\ H_2O \rightarrow S(An,nH) + UO_2 + 1/4nO_2 \quad (1)$$

This charge compensation mechanism is consistent with previous studies on actinide incorporations.[30] Therefore, we consider this mechanism as the preferred one for incorporation of V-, IV- and III-valent species. These configurations are presented in Fig. 3. The incorporation energies of Np and Am in

different oxidation states into both studtite and metastudtite are given in Table 4. In both cases the uranyl was substituted with $[NpO_2]^+$ and $[AmO_2]^+$ groups with adding hydrogen to balance the charge. We assumed the preferred charge-balancing mechanism to be the addition of hydrogens to actinyl group. Previously calculated results of Np incorporation into studtite by Shuller et al. [30] are included for comparison. The computed energy of incorporating Np into studtite is positive and large, which explains experimental difficulty in incorporating significant amount of Np into this phase. When considering the same reaction Shuller et al.[30] found that the formation of Np(VI) is preferred over formation of Np(V) in studtite; our calculations confirm this trend indicating that formation Np(VI) is preferable by ~0.3 eV. Interestingly, our results suggest that it should be slightly easier to incorporate Np(VI) into metastudtite than studtite, for which there is no experimental verification. The calculations for Am indicates that although it is much easier to incorporate Np(VI) than Am(VI) into both phases, the energy of incorporation of Am(IV) and Am(III) is smaller than that of Am(VI), indicating the preference of absorption of Am(IV)/Am(III). Interestingly, we again found that

Table 4. The energy (in eV) of Np and Am incorporation into studtite and metastudtite.

Actinide	Incorporation energy (eV) for		
	studtite	studtite[30]	metastudtite
Np(VI)	1.12	1.79	1.08
Am(VI)	2.21		2.18
Np(V)	1.43	2.49	1.35
Am(V)	2.50		2.51
Np(IV)	2.35		2.12
Am(IV)	1.95		1.64
Np(III)	3.39		2.97
Am(III)	2.01		1.47

incorporation of Am(III) into metastudtite is more energetically favourable than in studtite. These results are also supported by partial electronic density of states provided in Fig. S1 (Suplementary materials), which show stronger bounding of Am(III) than Am(V) and Am(V) in metastudtite than studtite.

As a final point, the energies reported in Table 4 indicate that the incorporation of both Np and Am are endothermic and that it should be harder to incorporate Am than Np into the considered phases. This trend could be also understood from the ionic radii of the considered cations. The replaced U(VI) cation in 8-fold configuration has radius of 0.86A, and Np(VI) to Np(IV) have similar size (0.83A-0.87A).[31] On the other hand, Am(III) is much larger (1.09A),[31] which explains more difficulty to incorporate Am than Np into studtite or metastudtite. This is in line with analysis of SNF that show Am and Cm are not incorporated whereas Np is.[32]

In order to explain our experimental results, we then suspended a sample containing Am in water for one month. The solid was separated and both phases analysed by gamma spectrometry and emission spectroscopy. There was no emission at room temperature and 77 K, suggesting that we had expelled the Am. To explore this effect more detail, we examined the photophysics at 8 K (Fig X), as we have previously used this to characterise studtite.[36] The results confirm the loss of the emission signal due to americium and that the material left shows a profile of the uranyl ion, that is similar to studtite, but less resolved. The average vibronic band spacing of 850 cm^{-1} is slightly lower than in studtite (878 cm^{-1}), measured under the same conditions. Time-resolved luminescence spectra at delay times up to 4 ms showed that the primary spectral features remained at all delay times, indicating one uranyl environment. Whilst the lifetimes of the emission are not so diagnostic at these low temperatures, two components can be fitted to the data (τ = 732±65 µs and 233±33 µs) that again have some similarities to studtite (862 µs (dominant) and 143 µs).

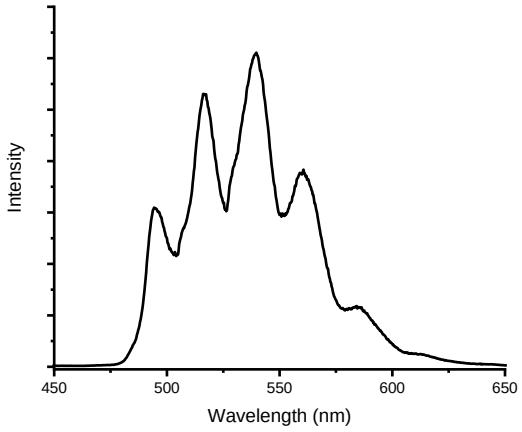

Figure X. Solid state emission spectrum of Am-incorporated studtite after washing, measured at 8 K (λ_{ex} = 415 nm)

Conclusions

Contacting studtite with Am(V) solutions or synthesising studtite in the presence of Am(V) gives rise to a product that does include Am but, from emission and vibrational spectroscopy, its likely in its +3 oxidation state. This is in contrast to the reactions of studtite with Am(III) where no Am is included in the structure. Theoretical calculations show that Am and Np can be incorporated into the structure of studtite and metastudtite, but as these incorporation energies are large and positive, it indicates that it would be difficult to incorporate these, which follows the experimental trends. Moreover, once in the structure, we have shown experimentally that they are easy to remove.

Experimental

Caution! Although depleted uranium was used during the course of the experimental work, as well as the radiological hazards uranium is a toxic metal and care should be taken with all manipulations. ^{241}Am is an α and γ emitter, and all experiments were carried out in a laboratory designated for the use of radioactive isotopes. Experiments using radioactive materials were carried out using pre–set radiological safety precautions in accordance with the local rules of Trinity College Dublin.

Raman spectra were obtained using 785-nm excitation on a Renishaw 1000 micro-Raman system. Carrier-free $^{241}AmCl_3$ (Perlamar) were obtained commercially. The Am-241 measurements were carried out by high-resolution gamma spectrometry using an n-type high-purity germanium detector (EG&G Ortec model GMX-15190) with a relative efficiency of 19% and a resolution of 1.90 keV (FWHM) at 1.33 MeV; this gives a total error of 15% in the measurements. The activities calculated as described in reference 33. The instrumentation and experimental procedures for luminescence spectroscopic measurement at near liquid helium temperature have been described previously. [34] Briefly, crystalline grains of the minerals were placed in 2 mm x 4 mm x 30 mm fused quartz cuvettes, capped with silicone stoppers, and then attached to the cold finger of a CryoIndustries RC152 cryostat with liquid helium vaporizing beneath the sample to reach a temperature of 8 ± 2 K. Time-resolved luminescence emission spectra of the samples were acquired by excitation at 415 nm with a Spectra-Physics Nd:YAG laser pumped Lasertechnik-GWU MOPO laser. The emitted light was collected at 85˚ to the excitation beam, dispersed through an Acton SpectroPro 300i double monochromator spectrograph, and detected with a thermoelectrically cooled Princeton Instruments PIMAX intensified CCD camera that was triggered by the delayed output of the laser pulse and controlled by the WinSpec data acquisition software. The photoluminescence decay curves were constructed by plotting the spectral intensity of a series of time-delayed luminescence spectra as a function of the corresponding delay time. The emission spectra and decay data were analysed using commercial software, IGOR®, from Wavematrix, Inc. X-ray powder diffraction patterns were recorded on a Siemens D500 using a Bragg-Brentano geometry with step size of 0.02˚ at 16 s for studtite.

The calculations were performed using density functional theory-based plane-wave Quantum-ESPRESSO code. [35] The computational setup is similar to the one used in our previous studies of studtite and metastudtite. [36] The calculations were performed with PBEsol exchange-correlation functional [37] and ultrasoft pseudopotentials to mimic the presence of core electrons. [38] The structures of studtite and metastudtite were represented with 68 and 48 atoms supercells. To get the converged structures we applied plane energy cutoff of 50 Ryd and the calculations were performed using 2x3x3 Methfessel-Paxton k-point sampling of Brillouin zone. [39] In order to correctly account for the 5f electrons correlations we applied DFT+U but with the Hubbard *U* parameter derived *ab initio*. Following our previous studies [29, 40] we applied the following Hubbard *U* parameter values: 2.6 eV for U, 3.1 eV for Np and 2.5 eV for Am.

Conflicts of interest

There are no conflicts to declare.

Acknowledgements

SB thanks the Irish Research Council for the award of a Government of Ireland Postdoctoral Fellowship. Part of this work was conducted at the William R. Wiley Environmental Molecular Sciences Laboratory (EMSL), a national scientific user facility located at the Pacific Northwest National Laboratory (PNNL) and sponsored by the Department of Energy's Office of Biological and Environmental Research (BER).

Notes and references

1 EC 2011, council directive 2011/70/euratom, official journal of the European union, L199/48, Feb 8, 2011.
2 A. Mesbah, S. Szenknect, N. Clavier, J. Lozano-Rodriguez, C. Poinssot, C. Den Auwer, R. C. Ewing and N. Dacheux, *Inorg. Chem.,* 2015, **54**, 6687.
3 R. J. Baker, *Coord. Chem. Rev*., 2014, **266–267**, 123.
4 J. P. Kaszuba and W. H. Runde, *Environ. Sci. Technol.*, 1999, **33**, 4427.
5 (a) P. C. Burns, K. M. Deely and S. Skanthakumar, *Radiochim. Acta,* 2004, **92**, 151; (b) A. L. Klingensmith, K. M. Deely, W. S. Kinman, V. Kelly and P. C. Burns, *Am. Miner.,* 2007, **92**, 662; (c) M. Douglas, S. B. Clark, J. I. Friese, B. W. Arey, E. C. Buck, B. D. Hanson, S. Utsunomiya and R. C. Ewing, *Radiochim. Acta,* 2005, **93**, 265.
6 (a) A. L. Klingensmith and P. C. Burns, *Am. Miner.,* 2007, **92**, 1946; (b) D. S. Alessi, J. E. S. Szymanowski, T. Z. Forbes, A. N. Quicksall, G. E. Sigmon, P. C. Burns and J. B. Fein, *J. Nucl. Mater*., 2013, **433**, 233.
7 (a) N. A. Meredith, M. J. Polinski, J. N. Cross, E. M. Villa, A. Simonetti and T. E. Albrecht-Schmitt, *Cryst. Growth Des.,* 2013, **13**, 386; (b) L. C. Shuller, R. C. Ewing and U. Becker, *J. Nucl. Mater.,* 2013, **434**, 440; (c) L. C. Shuller, R. C. Ewing and U. Becker, *Am. Mineral*., 2010, **95**, 1151.
8 P. C. Burns, R. C. Ewing and M. L. Miller, *J. Nucl. Mater.,* 1997, **245**, 1.
9 S. E. Binney, C. H. Bloomster, H. R. Brager, C. A. Burgess, W. J. Gruber, G. F. Howden, A. J. Naser, L. G. Niccoli, A. W. Prichard, J. A. Rawlins, G. W. Reddick, W. W. Schulz, J. P. Sloughter, J. L. Swanson, J. W. Thorton, C. N. Wilson and D. E. Wood, Clean Use of Reactor Energy, Report WHC-EP-0268; Westinghouse Hanford Company, Richland, WA, **1990**.
10 W. Runde, in *Radionuclides in the Environment*, *Vol. 2* (Ed.: D. A. Atwood,), John Wiley & Sons, Ltd, Weinheim, 2010, 315.

11 For a recent review see: H. Geckeis, J. Lützenkirchen, R. Polly, T. Rabung and M.Schmidt, *Chem. Rev.,* 2013, **113**, 1016.
12 S. Biswas, R. Steudner, M. Schmidt, C. McKenna, L. L. Vintro, B. Twamley and R.J. Baker, *Dalton Trans.*, 2016, **45**, 6383
13 C. Mallon, A. Walshe, R. J. Forster, T. E. Keyes and R. J. Baker, *Inorg. Chem.,* 2012, **51**, 8509.
14 B. McNamara, B. Hanson, E. Buck and C. Soderquist, *Radiochim. Acta,* 2005, **83**, 169.
15 K.-A. Hughes Kubatko, K.B. Helean, A. Navrotsky, and P.C. Burns, *Science*, 2003, **302**, 1191.
16 (a) K. -W. Kim, J. -T. Hyun, K. -Y. Lee, E. -H. Lee, K. -W. Lee, K. -C. Song and J. -K. Moon, *J. Hazard. Mater*. 2011, **193**, 52; (b) F. Clarens, J. de Pablo, I. Casas, J. Giménez, M. Rovira, J. Merino, E. Cera, J. Bruno, J. Quiñones and A. Martínez-Esparza, *J. Nucl. Mater.* 2005, **345**, 225; (c) F. Clarens, J. de Pablo, I. Díez, I. Casas, J. Giménez and M. Rovira, *Environ. Sci. Technol.,* 2004, **38**, 6656; (d) M.; Amme, B.; Renker, B.; Schmid, M. P.; Feth, H.; Bertagnolli, W. Döbelin, *J. Nucl. Mater.*, 2002, **306**, 202; (e) P. Diaz-Arocas, J. Quiñones, C. Maffiotte, J. Serrano, J. Garcia, J. R. Almazan, J. Esteban, *Mater. Res. Soc. Symp. Proc.* 1994, **353**, 641.
17 Y. Wang, K. von Gunten, B. Bartova, N. Meisser, M. Astner, M. Burger and R. Bernier-Latmani, *Environ. Sci. Technol.* 2016, **50**, 12266.
18 See for example: (a) T. Z. Forbes, P. Horan, T. Devine, D. McInnis, P. C. Burns, *Am. Miner.,* 2011, **96**, 202; (b) K.-A. Kubatko, D. Unruh, P. C. Burns, *Mater. Res. Soc. Symp. Proc.,* 2006, **893**, 423.
19 (a) J. Giménez, X. Martínez-Lladó, M. Rovira, J. de Pablo, I. Casas, R. Sureda, A. Martínez-Esparza, *Radiochim. Acta* 2010, **98**, 479; (b) R. Sureda, X. Martinez-Llado, M. Rovira, J. de Pablo, I. Casas, J. Gimenez, *J. Haz. Mat.*, 2010, **181**, 881.
20 M. Douglas, S. B. Clark, J. I. Friese, B. W. Arey, E. C. Buck and B. D. Hanson, *Environ. Sci. Technol.*, 2005, **39,** 4117.
21 W. H. Runde and B. J. Mincher, *Chem. Rev.*, 2011, **111**, 5723.
22 J. Gimenez, J. de Pablo, I. Casas, X. Martinez-Llado, M. Rovira and A. Martinez Torrents, *Appl. Geochem.*, 2014, *49*, 42.
23 REF
24 J. R. Bartlett and R. P. Cooney, *J. Mol. Struct.*,1989, **193,** 295.
25 P. C. Burns and K.-A. Hughes, *Am. Miner.*, 2003, **88**, 1165.
26 W. Runde, C. Van Pelt and P. G. Allen, *J. Alloys Compd.,* 2000, **303/304**, 182.
27 L.C. Shuller, R.C. Ewing and U. Becker, *Am. Mineral.*, 2010, **95**, 1151.
28 (a) L.C. Shuller, R.C. Ewing and U. Becker, *J. Nucl. Mater*. 2013, **434**, 440; (b) L. C. Shuller-Nickles, W. M. Bender, S. M. Walker and U. Becker, *Minerals* 2014, **4**, 690.
29 G. Beridze, A. Birnie, S. Koniski, Y. Ji and P.M. Kowalski, *Prog. Nucl. Energy*, 2016, **92**, 142.
30 (a) L.C. Shuller, R.C. Ewing and U. Becker, *J. Nucl. Mater*. 2013, **434**, 440; (b) L. C. Shuller-Nickles, W. M. Bender, S. M. Walker and U. Becker, *Minerals* 2014, **4**, 690.
31 R. D. Shannon. Acta Crystallographica. (1976). A32, Pages 751-767.
32 B. McNamara, B. Hanson, E. Buck and C. Soderquist, *Radiochim. Acta,* 2005, **83**, 169.
33 G. Gilmore and J. Hemingway, *Practical Gamma Spectrometry,* John Wiley & Sons. Chichester, 1995.
34 Z. Wang, J. M. Zachara, P. L. Gassman, C. Liu, O. Qafoku, W. Yantasee and J. G. Catalano, *Geochim. Cosmochim. Acta,* 2005, **69**, 1391.
35 P. Giannozzi, S. Baroni, N. Bonini, M. Calandra, R. Car, C. Cavazzoni, D. Ceresoli, G. L. Chiarotti, M. Cococcioni, I. Dabo, A. Dal Corso, S. de Gironcoli, S. Fabris, G. Fratesi, R. Gebauer, U. Gerstmann, C. Gougoussis, A. Kokalj, M. Lazzeri, L. Martin-Samos, N. Marzari, F. Mauri, R. Mazzarello, S. Paolini, A. Pasquarello, L. Paulatto, C. Sbraccia, S. Scandolo, G. Sclauzero, A. P. Seitsonen, A. Smogunov, P. Umari and R. M. Wentzcovitch, *J. Phys.: Condens. Matter,* 2009, **21**, 395502.
36 T. Vitova, I. Pidchenko, S. Biswas, G. Beridze, P. W. Dunne, D. Schild, Z. Wang, P. M. Kowalski and R. J. Baker, *Inorg. Chem.*, 2018, **57**, 1735.
37 J.P. Perdew, A. Ruzsinszky, G.I. Csonka, O.A. Vydrov, G.E. Scuseria, L.A. Constantin, X. Zhou and K. Burke, *Phys. Rev. Lett.*, 2008, **100**, 136406.
38 D. Vanderbilt, *Phys. Rev. B: Condens. Matter Mater. Phys.* 1990, *41*, 7892.
39 M. Methfessel and A. T. Paxton, *Phys. Rev. B: Condens. Matter Mater. Phys.*, 1989, **40**, 3616.
40 G. Beridze and P.M. Kowalski, *J. Phys. Chem. A*, 2014, **118**, 11797.

